Original Paper

Nonaxisymmetric residual stress distribution in axisymmetric glass articles

Hillar Aben, Johan Anton and Jüri Josepson

Institute of Cybernetics, Estonian Academy of Sciences, Tallinn (Estonia)

Residual stress measurements in many bottles, tumblers and in other axisymmetric glass articles by using integrated photoelasticity have shown that the residual stress distribution often deviates from the axially symmetric one. A method is developed which enables determination of nonaxisymmetric residual stress distribution. A computer-controlled polariscope has been developed for automatic measurements. Several examples of residual stress distributions, which deviate strongly from the axisymmetric one, are given. It is shown that deviations from axial symmetry lead to less favorable distribution of the residual stresses; e.g., they may lead to tensile residual stresses on the external surface of bottles.

Nichtaxialsymmetrische Verteilung der Eigenspannungen in axialsymmetrischen Glasgegenständen

Die Messung von Eigenspannungen in vielen Flaschen, Trinkgläsern und anderen axialsymmetrischen Glasgegenständen mit der integralen Spannungsoptik hat gezeigt, daß die Verteilung der Eigenspannungen oft von der axialsymmetrischen Verteilung abweicht. Es wird ein Verfahren entwickelt, das die Bestimmung der nichtaxialsymmetrischen Spannungsverteilungen ermöglicht. Für die spannungsoptischen Messungen wird ein automatisiertes Polariskop konstruiert. Einige Beispiele für die Verteilung von Eigenspannungen, die erheblich von der axialsymmetrischen Verteilung abweichen, werden beschrieben. Es wird gezeigt, daß die Abweichung von der axialen Symmetrie eine ungünstigere Verteilung der Eigenspannungen verursacht; z.B. können auch auf der Außenfläche von Flaschen Zugspannungen auftreten.

1. Introduction

Integrated photoelasticity enables measurement of residual stresses in axisymmetric glass articles [1]. For that the specimen is placed in an immersion bath to avoid refraction of light, and observed in a polariscope (figure 1). The wall of the specimen AB is scanned in the section of interest, measuring the parameter of the isoclinic and the optical retardation. This procedure is named tangential incidence. Algorithms and computer programs have been elaborated which permit calculation of the axial and shear stress distribution through the wall of the specimen, assuming that the stress distribution is axisymmetric [1]. If stress gradients in the axial direction are absent or weak, also other stress components can be determined.

On investigating an axisymmetric glass article, the light can be passed through the latter perpendicularly to different meridional sections (figure 2). In the case of axisymmetric residual stress distribution, one should obtain for all measurements the same data (differing no more than the measurement errors), and interpretation of the latter should give similar stress distribution all over the perimeter.

Practical measurement of residual stress in many bottles, tumblers, and other glass articles has shown that mostly that is not the case. Almost always the residual stress distribution deviates from the axisymmetric one, often considerably. This is reflected in measurement data which also varies considerably around the perimeter.

Experience shows that it is completely possible to carry out integrated photoelastic measurements also in the case when stresses vary around the perimeter. The stresses which are determined should be related to the meridional section, perpendicular to which the light is passed through the specimen.

Approximate values of the stresses can be calculated using the algorithm which is based on the assumption that the stress distribution is axisymmetric. There is no controversy in this statement, e.g., if stresses vary symmetrically relative to the meridional section measured, the measurement data corresponds exactly to the stresses in the meridional section. However, with a more complicated variation of stresses around the perimeter the simplified algorithm may not be sufficiently precise. Due to this, calculated stresses near the maxima are to

Received April 27, 1995, revised manuscript July 10, 1995.

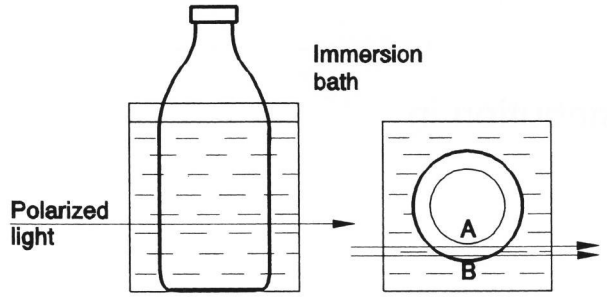

Figure 1. Investigation of an axisymmetric glass article by tangential incidence.

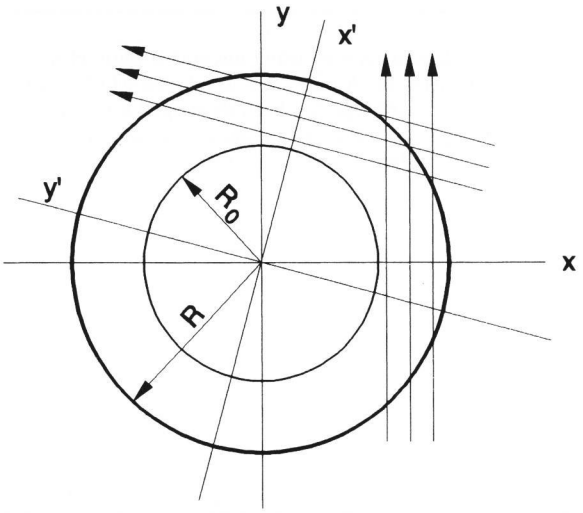

Figure 2. At measurements the light can be passed through the article perpendicularly to different meridional sections.

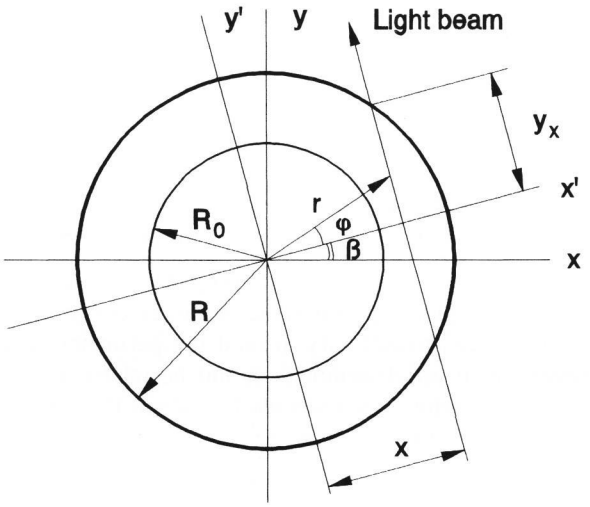

Figure 3. Geometrical notations for tangential incidence.

a certain extent diminished, and near the minima increased.

Therefore, an algorithm has been developed for calculation of the stresses by using measurement data, which is free from the assumption about axial symmetry.

2. Algorithm for determining nonaxisymmetric stresses in axisymmetric hollow glass articles

The case when the stress gradient in the direction of the z axis (axis of the article) is absent or weak is now considered. In this case the only stress component which influences the polarization of light is the axial stress σ_z. Assuming that stresses vary both in radial and circumferential directions, σ_z can be presented as (figure 3)

$$\sigma_z(\varrho, \beta) = f_0(\varrho) + \sum_{m=1}^{M} [f_m^c(\varrho) \cos m\beta + f_m^s(\varrho) \sin m\beta] , \quad (1)$$

where the angle β is shown in figure 3, and $\varrho = r/R$.

Integral Wertheim law [1] gives

$$\delta = C \int_{-y_x}^{y_x} \sigma_z \, dy , \quad (2)$$

where δ is the optical retardation, and C is the photoelastic constant. Functions $f_0(\varrho)$, $f_m^c(\varrho)$, and $f_m^s(\varrho)$ can be expressed as power series

$$f_0(\varrho) = \sum_{k=0}^{K} c_{2k} \varrho^{2k}, \quad f_m^c(\varrho) = \sum_{k=1}^{K} a_{2k} \varrho^{2k}, \quad f_m^s(\varrho) = \sum_{k=1}^{K} b_{2k} \varrho^{2k}, \quad (3)$$

where a_{2k}, b_{2k} and c_{2k} are the coefficients to be determined from the measurement data.

Inserting equation (1) into equation (2),

$$\frac{\delta(\xi, \beta)}{CR} = \sum_{k=0}^{K} c_{2k} G_{2k} + \sum_{m=1}^{M} \sum_{k=1}^{K} (a_{2k} \cos m\beta + b_{2k} \sin m\beta) I_{2k}^m \quad (4)$$

is obtained, where $\xi = x'/R$, and

$$G_{2k} = \xi^{2k+1} \int_{-\arccos\xi}^{\arccos\xi} \frac{1}{\cos^{2k+2}\varphi} \, d\varphi , \quad (5)$$

$$I_{2k}^m = \frac{\xi^{2k+1}}{\cos m\beta} \int_{-\arccos\xi}^{\arccos\xi} \frac{\cos m(\beta + \varphi)}{\cos^{2k+2}\varphi} \, d\varphi . \quad (6)$$

The functions G_{2k} and I_{2k}^m can be written in the following form

$$G_0 = 2\sqrt{1 - \xi^2} , \quad (7)$$

$$G_{2k} = \frac{1}{2k+1} G_0 + \frac{2k}{2k+1} G_{2k-2} , \quad (8)$$

$$I_0^1 = 2\xi \ln \frac{1 + \sqrt{1 - \xi^2}}{\xi} , \quad (9)$$

$$I_{2k}^1 = \frac{2k-1}{2k} I_{2k-2}^1 + \frac{1}{k} \xi \sqrt{1 - \xi^2} , \quad (10)$$

$$I_0^2 = 4\xi \cos\xi - G_0 , \quad (11)$$

$$I_{2k}^2 = 2\xi^2 G_{2k-2} - G_0 , \text{ etc.} \quad (12)$$

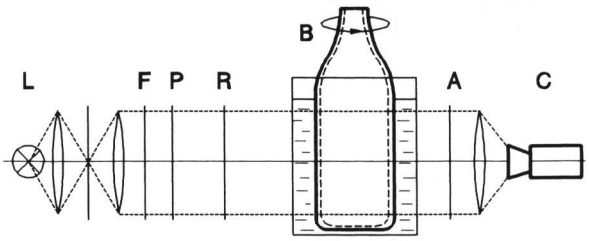

Figure 4. Optical system of polariscope. L: light source, F: filter, P: polarizer, R: retarder, B: bottle in immersion bath, A: analyzer, C: CCD camera.

Equation (4) should be considered as an overdetermined system of equations from which the coefficients a_{2k}, b_{2k} and c_{2k} can be determined by using the method of least squares. It is assumed that for the sake of precision the number of measurement data $\delta(\xi, \beta)$ is larger than the number of unknown coefficients.

If variation of the stresses over the perimeter is ignored, only the first terms in equations (1 and 4) are taken into account. This leads to the algorithm for the axisymmetric case [1].

3. Measurement apparatus

Since wall thickness of glass articles is often only several millimeters or even less, for photoelastic measurements one needs a polariscope for pointwise measurements with 10 magnifications at least. The coordinate device should enable to record the horizontal coordinate of the measurement point with a precision of 0.01 mm and the polariscope should be supplied with a compensator for precise measurement of the optical retardation. Such a polariscope has been described in [2]. For determining residual stress distribution in a section of a glass article for a certain value of the angle β (figure 3), one has to measure the optical retardation at least at 6 to 10 values of the coordinate x. With the manual polariscope this takes about 5 min. That is in usual factory conditions completely admissible.

However, for more complete analysis of the stresses, including stress distribution over the perimeter, one may use an automatic polariscope. Figure 4 shows basic components of the optical system of an automated polariscope. Before entering the immersion bath polarized light passes an optical retarder R with a set of parallel horizontal fringes. Due to stresses in the wall of the specimen, these fringes are deformed and recorded by the CCD (Charge-Coupled Device) camera C. In this version the automatic polariscope enables quick measurement of the axial stress distribution through the wall of the specimen if stress gradient in the axial direction and birefringence in the article are weak.

Information from the optical block (from the CCD camera) is fed into the frame grabber which is located in the PC. A software package has been developed which calculates stresses in the section where measurements were made. After the photoelastic measurements in a position of the article are made, it is turned by a stepper engine for a certain angle $\Delta\beta$, and again the photoelastic measurements and stress calculation are carried out. Stress distribution through the wall at any value of β as well as distribution of the surface stresses over the perimeter can be shown on the monitor.

If the bottle is under internal pressure, the value of the latter is also calculated. The algorithm for that is based on the fact that since residual stresses must be in equilibrium over the section, the resulting axial force in the bottle is caused by internal pressure.

4. Comparison of the stress calculation algorithms

One important indicator of the residual stresses in a glass article is the distribution of the average through-wall (membrane) axial stress over the perimeter. This

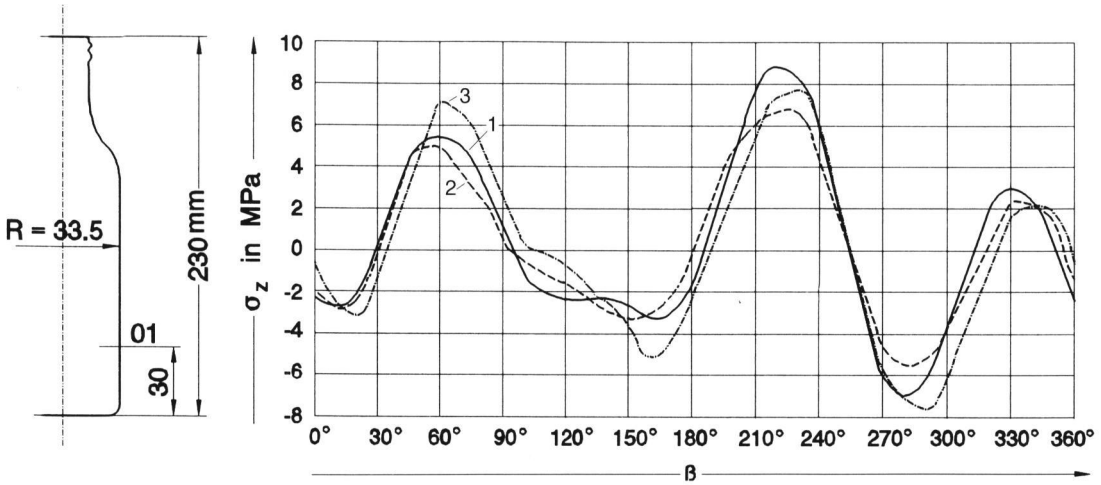

Figure 5. Geometry of the 0.5 l bottle and distribution of the axial membrane stress in section 01 over the perimeter. Curve 1: exact algorithm, curve 2: local interpretation of the measurement data obtained by tangential incidence, curve 3: using normal incidence.

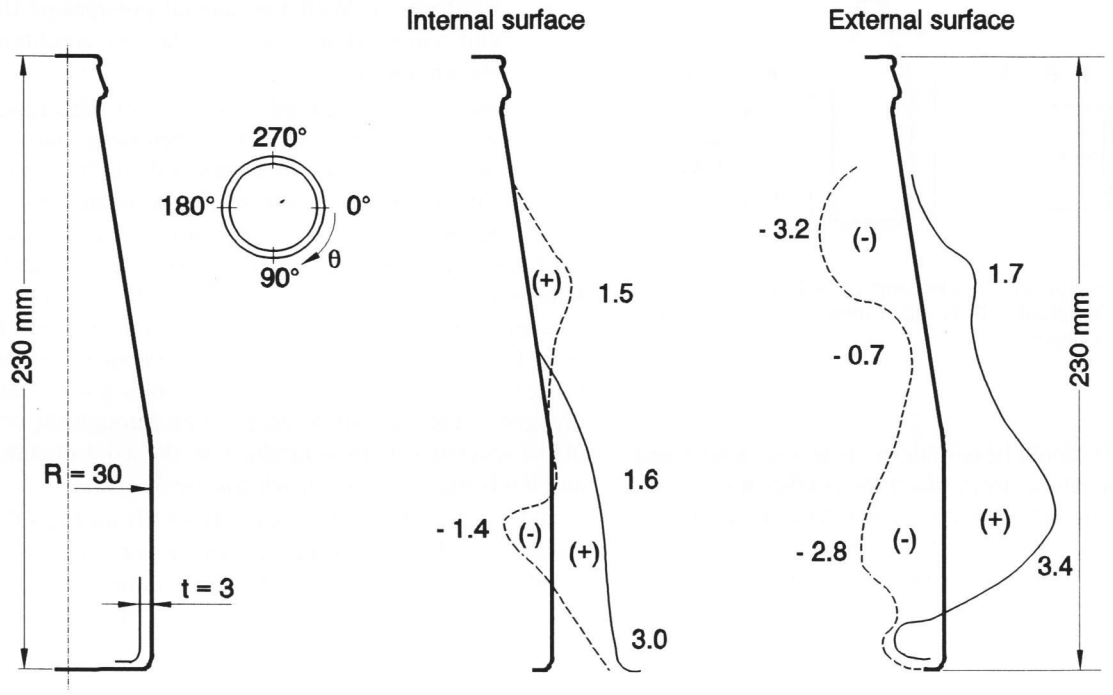

Figure 6. Geometry of the beer bottle and distribution of the meridional stress σ_z (in MPa) on the surfaces at two meridional sections. ——: $\beta = 225°$, – – –: $\beta = 300°$.

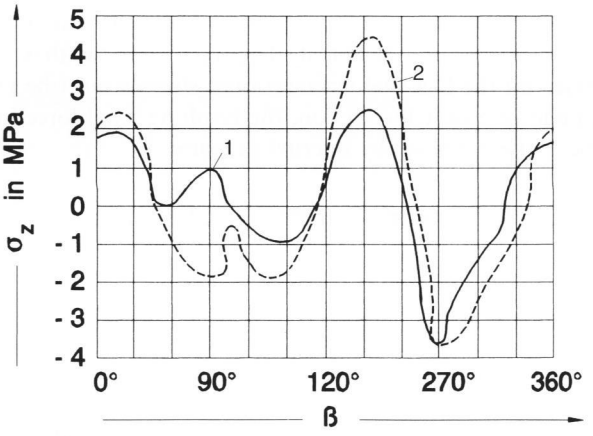

Figure 7. Distribution of the axial surface stresses over the perimeter at $z = 70$ mm in the beer bottle. Curve 1: internal surface, curve 2: external surface.

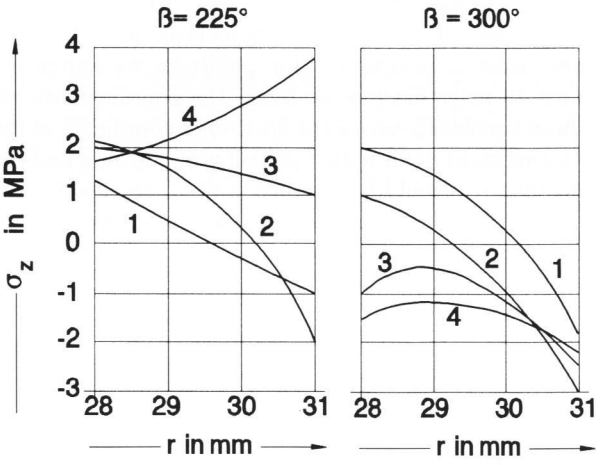

Figure 8. Distribution of the axial stresses through the wall for two meridional sections at different distances z from the bottom of the beer bottle. Curve 1: $z = 5$ mm, curve 2: $z = 15$ mm, curve 3: $z = 40$ mm, curve 4: $z = 70$ mm.

distribution may be measured by different methods. Firstly, by using tangential incidence, one may interpret the measurement data for a meridional section assuming that stress distribution is axisymmetric. Secondly, membrane stresses can be determined by using passage of light through the bottle wall in the direction of the normal to the latter (using a reflection polariscope). Thirdly, most precise results are obtained by using the algorithm described in section 2. of this paper.

Figure 5 shows the geometry of a 0.5 l bottle and the distribution of the axial membrane stress in section 01, obtained by using these three methods. It shows that also simplified interpretation of the measurement data gives rather satisfactory results. However, at the sections with extreme values of the stresses simplified methods give for the stresses somewhat diminished absolute values.

5. Examples

5.1 Beer bottle

In figure 6 the geometry of the bottle as well as the distribution of the meridional surface stresses for two meri-

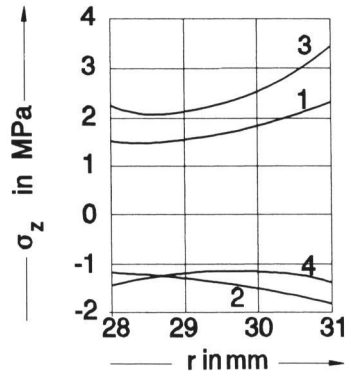

Figure 9. Distribution of the axial stresses through the wall at z = 70 mm for different meridional sections of the beer bottle. Curve 1: β = 0°, curve 2: β = 160°, curve 3: β = 225°, curve 4: β = 300°.

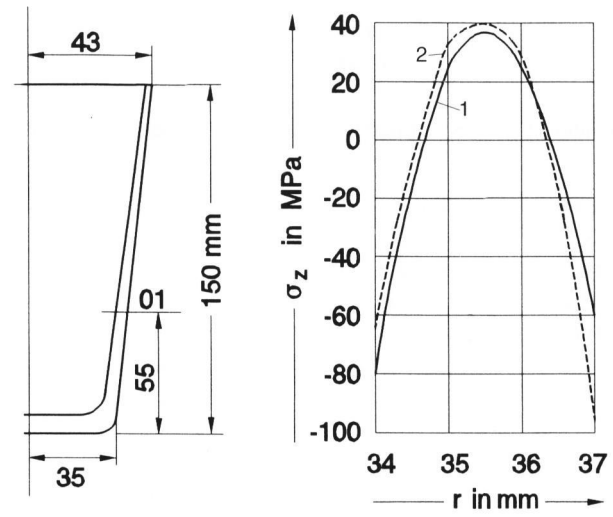

Figure 10. Geometry of the tumbler and distribution of the axial stress through the wall for two azimuths. Curve 1: β = 0°, curve 2: β = 135°.

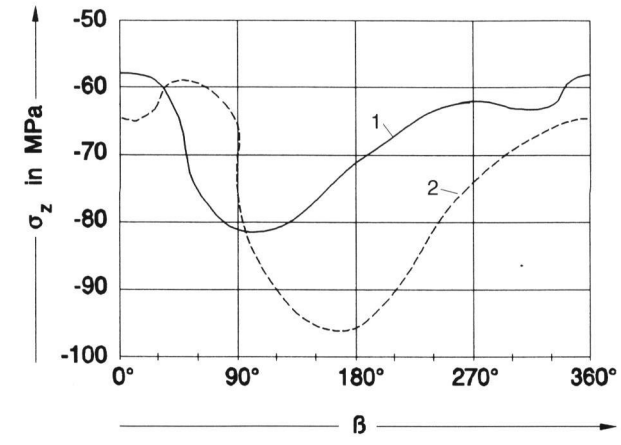

Figure 11. Distribution of the meridional surface stresses over the perimeter in the tumbler at z = 55 mm. Curve 1: internal surface, curve 2: external surface.

dional sections are shown. It is seen that stress distributions in the meridional sections β = 225° and β = = 300° differ drastically. At β = 225° both surfaces of the bottle are under tension.

Distribution of the axial meridional stress at the surfaces over the perimeter is shown in figure 7. It is seen that even at the external boundary tensile stresses appear in several regions over the perimeter.

Figure 8 shows distribution of the axial stress through the wall for two meridional sections at different distances from the bottom of the bottle. It is seen that when at z = 5 mm stresses in both meridional sections are almost in equilibrium, at z = 40 mm and z = 70 mm for β = 225° the stresses are tensile, and for β = 300° compressive through the whole wall.

Figure 9 shows distribution of the axial stress through the wall at z = 70 mm for different meridional sections.

Qualitatively similar results about the deviation of the stress distribution from the axisymmetric one have been obtained by the authors practically always when detailed measurements of the stresses in bottles have been carried out.

5.2 Tumbler

Figure 10 shows geometry of the tumbler and axial stress distribution at z = 55 mm for two values of β. In figure 11 the distribution of the meridional surface stresses over the perimeter at z = 55 mm is shown.

5.3 Electric lamp

The geometry of a lamp is shown in figure 12. The figure shows also distribution of the meridional surface stresses near the socket. Figure 13 shows the distribution of the meridional surface stresses over the perimeter of the lamp in section 3.

6. Discussion

Figure 14 shows typical residual stress distribution through the wall of a bottle. Due to more intensive cooling of the external surface the latter is under compression. The internal surface is under tension, the absolute value of which is usually lower than that of the stress on the external surface. If stress distribution is axisymmetric, the same stresses should be present in all the meridional sections. These stresses which are mostly caused by the temperature gradient through the wall are named thickness stresses [1].

Due to nonaxisymmetric cooling conditions an additional axial membrane stress field (figure 14) appears in the bottle. These stresses are not axisymmetric. In some regions of the perimeter they are tensile, in other parts compressive. These stresses are caused by the temperature gradient over the perimeter and they are named form stresses [2]. Total stresses are the sum of the thickness and form stresses, which is illustrated in figure 14.

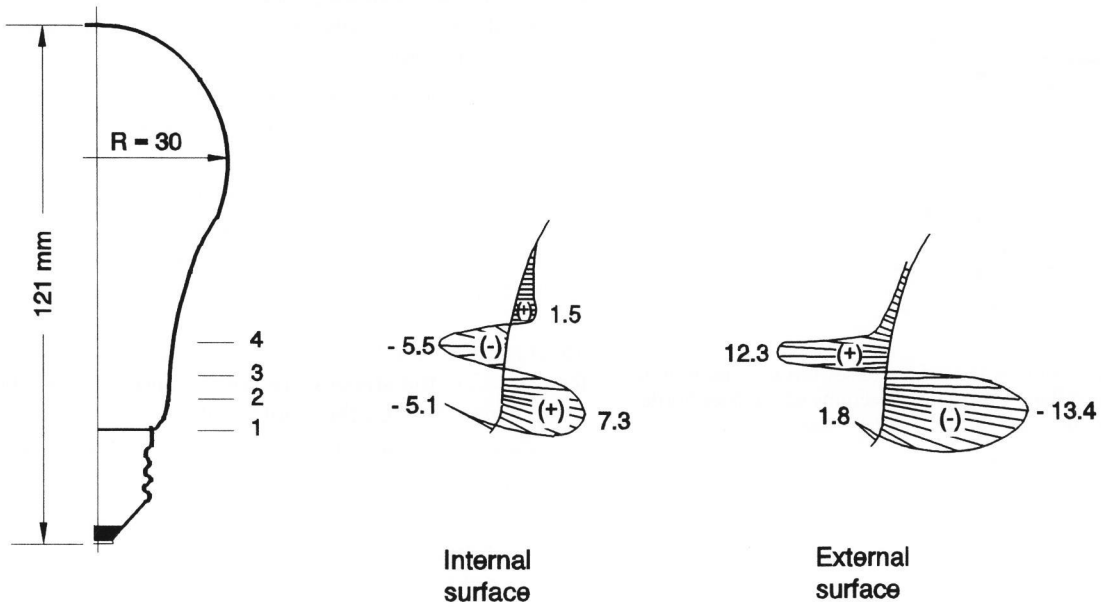

Figure 12. Geometry of the electric lamp and distribution of the meridional stresses σ_z (in MPa) on the surfaces near the socket.

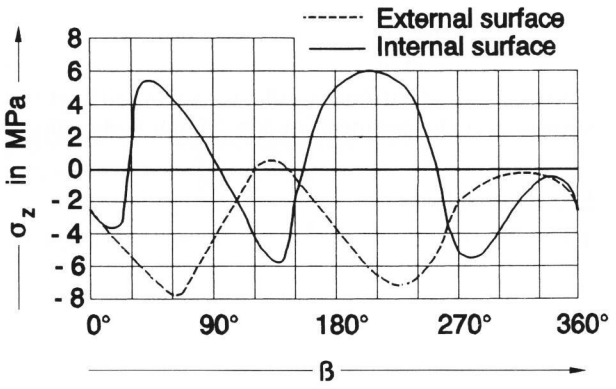

Figure 13. Distribution of the meridional surface stresses around the perimeter in section 3 of the electric lamp.

It is seen that in the case of tensile form stresses the total stresses may be positive even on the external surface of the bottle. This fact is confirmed by figures 7 to 9. Thus, due to deviation of the residual stress distribution from the axisymmetric one, tensile stresses may appear on the external surface of bottles, which increases the danger of their breaking.

In the case of the tempered tumbler (section 5.2), deviations of the stress distribution from the axisymmetric one cause variation of the compressive surface stresses over the perimeter decreasing their strength.

The reason for the deviation of the residual stress distribution from the axisymmetric one is probably the nonaxisymmetric temperature of the article during different stages of the production process as well as nonaxisymmetric cooling conditions. Significance of glass flow symmetry in the feeder bowl and possibilities to improve it have already been considered in the literature [2]. Thus, it is important to have an axisymmetric temperature distribution in the gob.

The next reason for nonaxisymmetric temperature distribution in the bottle may be the noneven temperature of the mold.

Thirdly, in the lehr cooling conditions for the article are not the same over the perimeter. In figure 15, the points A, B, C and D of the article in the middle cool down more quickly than other parts. This has been considered in [3] as the main reason for nonaxisymmetric residual stresses.

There may be other reasons for the nonaxisymmetric distribution of the residual stresses, e.g. variation of the residual stresses over the perimeter is related to the variation of the wall thickness over the perimeter.

7. Conclusions

The measurement of residual stresses in many axisymmetric glass articles by integrated photoelasticity has shown that deviation of the residual stress distribution from the axisymmetric one may be considerable. This deviation causes less favorable residual stresses in the articles and decreases the resistance of the latter. In annealed articles (like bottles) tensile stresses may appear even on the external surface of the articles.

To increase resistance of axisymmetric glassware it is desirable to analyze the reasons for the nonaxisymmetric residual stresses and to modify correspondingly the technology. Since integrated photoelasticity enables to meas-

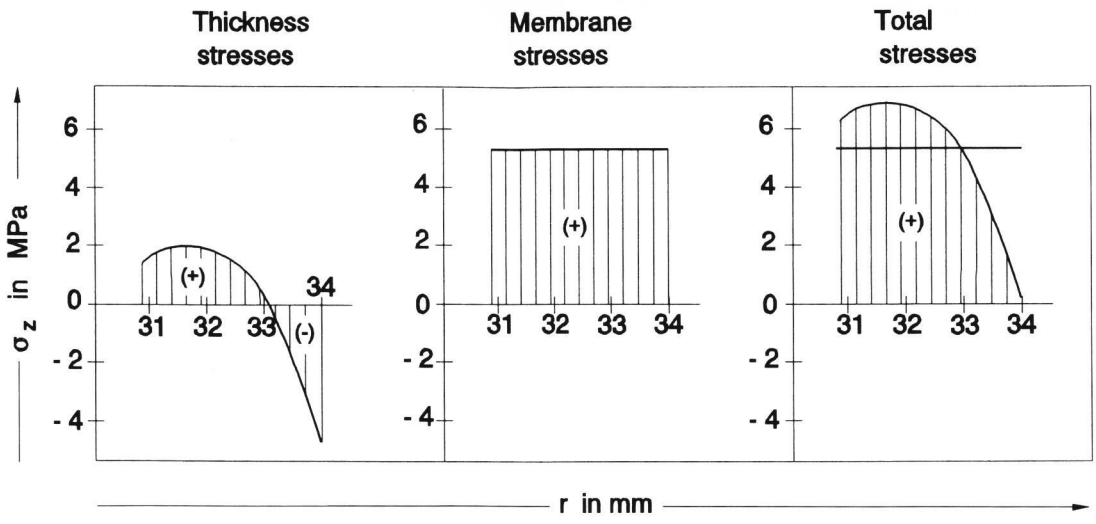

Figure 14. Total residual stresses consist of thickness stresses and membrane stresses.

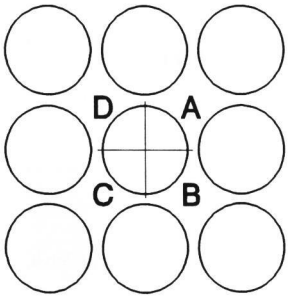

Figure 15. Position of axisymmetric glass articles in the lehr.

ure both axisymmetric and nonaxisymmetric residual stress distributions, it may help to optimize the manufacturing technology of axisymmetric glassware.

This paper shows also that stress calculation programs which are based on the assumption of axial symmetry of the stresses do not give the real residual stress distribution in axisymmetric glass articles.

8. Nomenclature

a_{2k}	coefficient of the polynomial approximation of $f_m^c(\varrho)$
b_{2k}	coefficient of the polynomial approximation of $f_m^s(\varrho)$
C	photoelastic constant in TPa^{-1}
$f_0(\varrho)$	coefficient in the stress expansion which does not depend on β
$f_m^c(\varrho)$	coefficient in the stress expansion before the term $\cos m\beta$
$f_m^s(\varrho)$	coefficient in the stress expansion before the term $\sin m\beta$
G_{2k}	known functions of ξ
I_{2k}^i	known functions of ξ
K	total number of terms
k	current number
M	total number of terms
m	current number
R	external radius of the specimen in mm
R_0	internal radius of the specimen in mm
r	radial coordinate in mm
x	space coordinate perpendicular to the light ray
y	space coordinate parallel to the light ray
z	space coordinate in the direction of the axis of the specimen
β	angle which determines the direction of the light beam
$\Delta\beta$	step of β
δ	optical retardation in nm
$\xi = x/R$	dimensionless coordinate
$\varrho = r/R$	dimensionless radial coordinate
σ_r	radial stress in MPa
σ_z	axial stress in MPa
σ_θ	circumferential stress in MPa
φ	circumferential coordinate

9. References

[1] Aben, H.; Guillemet, C.: Photoelasticity of glass. Berlin (et al.): Springer 1993.

[2] Stanley, M.: Modelling for a new feeder bowl. Glass Technol. **35** (1994) no. 1, p. 22–26.

[3] Belousov, Y. L.: Effect of annealing of vials on glass dust contamination of medical preparations. Glass Ceram. **49** (1992) no. 9, p. 438–440.

Address of the authors:
H. Aben, J. Anton, J. Josepson
Institute of Cybernetics, Estonian Academy of Sciences
21, Akadeemia tee, EE-0026 Tallinn (Estonia)